Influence of chemical compositions and molecular weights of humic acids on Cr(VI) photo-reduction

S.Y. Chen[a], S.W. Huang[a], P.N. Chiang[b], J.C. Liu[c], W.H. Kuan[d], J.H. Huang[a], J.T. Hung[e], Y.M. Tzou[a,*], C.C. Chen[f], M.K. Wang[g]

[a] Department of Soil & Environmental Sciences, National Chung Hsing University, Taichung, 40227 Taiwan, ROC
[b] The Experimental Forest, National Taiwan University, Nantou, 55743 Taiwan, ROC
[c] Agricultural Research Institute No. 189, Jhongjheng Rd., Wufong, Taichung County, 41301 Taiwan, ROC
[d] Department of Safety, Health, and Environmental Engineering, Ming Chi University of Technology, Taishan, Taipei, 24301 Taiwan, ROC
[e] Department of Horticulture, National Taitung Junior College, Taitung, 95045 Taiwan, ROC
[f] Department of Life Science, National Taiwan Normal University, Taipei, 116 Taiwan, ROC
[g] Department of Agricultural Chemistry, National Taiwan University, Taipei, 10617 Taiwan, ROC

ARTICLE INFO

ABSTRACT

Humic acids (HA) strongly affect the fate of trace metals in soils and aquatic environments. One of the remarkable properties of HA is its ability to reduce Cr(VI), an extremely toxic anion. However, it is unclear which HA components are involved in Cr(VI) reduction and possess the photo-induced properties. In this study, an ultrafiltration technique was used to fractionate HAs into four fractions of different nominal molecular weights (M_w): >100, 50–100, 10–50 and <10 kDa. Each HA fraction was characterized by spectroscopic analyses followed by examining Cr(VI) removal on each fraction of HA at pH 1–5. Spectroscopic results indicated that low-M_w HA was enriched with polar and aromatic domains. These polar, including polar C in aliphatic region, and aromatic groups were the major sites for Cr(VI) reduction because they disappeared rapidly upon interaction with Cr(VI). As a result, low M_w of HA exhibited greater efficiency of Cr(VI) reduction. Light induced the rapid transfer of electrons between chromate-phenol/carboxyl ester, or the formation of peroxide radicals or H_2O_2 through the ready decay of peroxy radicals associated with polar substituents, explained the rapid scavenging of Cr(VI) on polar and aromatic groups of HAs under illumination.

© 2011 Elsevier B.V. All rights reserved.

1. Introduction

Soil organic matter (SOM) consists of two major components, unaltered debris and humus, which are defined as a recognizable skeleton and an invisible feature of its original organism, respectively. Humus is an amorphous brown-colored polymer, which can be subdivided according to solubility in strong acid and base: humic acid (HA, insoluble in acid), fulvic acid (FA, soluble in both acid and base) and humin (insoluble in both acid and base). These humic substances (HS) strongly affect the fate of trace metals and organic contaminants in terrestrial and aquatic environments through various binding and degrading processes, including photo-chemical reactions [1–4]. Because HS have complex chemical compositions with molecular weight (M_w) ranges of hundreds to several hundred thousand Daltons, fractionation of HS is an effective method for better insight into the characters of HS and their interactions with pollutants [5].

It has been observed that the chemical composition and total acidity of HAs differed greatly between high and low M_w fractions [6]. With the fractionation of an Andisol HA by coupling size exclusion chromatography (SEC) and polyacrylamide gel electrophoresis (PAGE), Richard et al. [7] found that carboxylic groups could be concentrated in low M_w fractions, while polysaccharides and peptides were in high M_w fractions, and the UV–vis absorbance and A_{465}/A_{665} ratio increased as M_w of HA decreased. Christl and Kretzschmar [8] used a hollow fiber ultrafiltration (UF) technique to fractionate HA into four M_w: 10–30, 30–100, 100–300 and >300 kDa. They observed that the negative charge of HA decreased steadily with increasing M_w fractions over a pH range of 3–10 in a 0.1 M background electrolyte, and the decrease was consistent with the decrease of phenolic and carboxylic C in HA. Moreover, high M_w fractions exhibited generally lower photo-inductive activities and weaker fluorescence emission compared to low M_w fractions and bulk HAs [5,9]. These studies clearly demonstrated that the major functional groups and the properties of chromophores depended greatly on the M_w of HAs.

* Corresponding author at: Department of Soil and Environmental Sciences, 250 Kuo-Kuang Rd., Taichung, 40227 Taiwan, ROC. Tel.: +886 4 22840373x4206; fax: +886 4 22855167.
E-mail address: ymtzou@dragon.nchu.edu.tw (Y.M. Tzou).

Therefore, the HAs of various M_w should exhibit different chemical reactivities, including photo-induced abilities, when in contact with environmental pollutants. The activated sites on HAs may be identified upon their enrichment through a fractionation of HAs into various M_w prior to interactions of pollutants.

HS serve as electron donors in many redox reactions. In particular, the elimination of environment pollutants such as Cr(VI) by HA have received much scientific attention [10–13]. Cr(VI) is toxic to both plants and animals [14,15] and is carcinogenic to human beings [16]. Therefore, the conversion of Cr(VI) to less toxic Cr(III) by HS can eliminate its hazard to organisms, and the redox reaction is considered a self-cleaning function in Cr(VI)-loaded environments. The interactions of Cr(VI) with HA have been investigated in many previous studies [11,17]; however, which functional groups of HAs participate in Cr(VI) reduction remains unknown. The utilization of bulk HA, bearing extremely complex structures, as a reactant may inhibit the detailed observations of the activated groups of HA involved in Cr(VI) reduction. Thus, fractionating HAs into different M_w with dominant chemical compositions may facilitate mechanistic studies of Cr(VI) reduction on HAs. Photo-induced Cr(VI) reduction by HA may occur in an environment receiving sunlight and thus, the investigation of photo-detoxification of Cr(VI) by HA can help delineate the overall Cr(VI) behavior in ecosystems. In this study, HA was obtained from a mountain peat soil of Taiwan, and fractionated into four M_w (i.e. <10, 10–50, 50–100 and >100 kDa) using UF technique. The adsorption and photo-reduction of Cr(VI) by different M_w of HAs were investigated and the specific groups of HAs involved in Cr(VI) removal were also evaluated. The experiments were conducted at pH 1–5; nonetheless, Cr(VI) reduction by HA proceeded slowly at a higher pH, and thus, we mainly presented a representative result obtained at pH 1. In addition, an extremely acidic effluent with Cr(VI) derived from electroplating industries had been detected in an open irrigation ditch or a river closed to the discharging points [18]. Therefore, the current experimental results can demonstrate the interactions of HA with Cr(VI) in a natural system.

2. Materials and methods

2.1. The source of HAs

A peat soil sample was collected from the Yangmingshan Mountain area located in Taipei County, northern Taiwan (25°090N, 121°320E, Fig. 1). The Yangmingshan soil contains 156 g/kg organic carbon (OC), and is classified as medial, amorphic, thermic, Typic Melanudand. Other physical/chemical properties of the peat soil can be found in our previous work [19].

2.2. Extraction and fractionation of HAs

HAs were extracted from the peat soil, following the standard procedure recommended by the International Humic Substances Society (IHSS) [19]. The HA samples were transferred to a solution with 0.1 M NaOH and 0.01 M NaCl at pH 7, and were passed through membranes with nominal molecular weight cut-offs (MWCO) of 100, 50 and 10 kDa using a Molecular Stirred Cell (Molecular/Porÿ Stirred Cells, S-76–400). The separation was carried out stepwise under a pressure of 16 psi, beginning with the highest MWCO, and the filtrate passing through the membrane was collected and transferred to the next membranes with a lower MWCO for separation. Each HA size-fraction obtained was stored in a dark glass bottle as a stock solution and placed in a refrigerator for further use.

2.3. Characterization of HA fractions

The elemental contents (C, H, N and O) of the HA fractions were investigated by a Heraeus CHNOS Rapid F002 Elemental Analyzer.

The optical densities ratios of dilute HA solutions at 465 and 665 nm (E_4/E_6) were evaluated according to the method of Chen et al. [20]. ^{13}C CP-MAS NMR spectra and infrared spectra of HA fractions were obtained using a Bruker DSX400WB NMR spectrometer and Fourier Transform Infrared (FTIR) Spectrometer (Thermo Nicolet NEXUS), respectively. ^{13}C CP-MAS NMR spectra of the samples were collected on a Bruker DSX400WB NMR spectrometer [19]. Spectroscopic analyses of the specific functional groups of HA involved in Cr(VI) reduction was obtained by comparing the changes in the spectra of Cr(VI)-loaded HA with the untreated HA samples. A control experiment was also conducted by mixing Cr(III) [i.e. CrCl$_3$] up to 9.62 mM with untreated HA samples to evaluate the possible complexation of the redox products, i.e., Cr(III), on spectroscopic analyses.

2.4. Cr(VI) reduction by various M_w of HA

Appropriate amounts of the stock solution of each HA fraction was diluted with 0.001 M CaCl$_2$ to obtain a C concentration of ≈ 52 mg L^{-1}, measured by TOC analyzer. A small aliquot of Cr(VI) stock solution (1.923 mM) was diluted with 0.001 M CaCl$_2$ and then transferred to a water-jacketed reaction vessel containing HA. Consequently, the final concentration of Cr(VI) was 0.1923 mM, and the final HA concentration was 26 ± 2 mg C L^{-1}. Cr(VI) reduction by HA was conducted in 1 L reaction vessel at pH 1–5, and a circulating water bath connected to the vessel to maintain the reaction temperature at 25 ± 1 °C. A 100 W medium-pressure mercury UV lamp (ACE Glass Incorporated) was inserted into a borosilicate well to exclude the irradiation from UVB and placed in the center of the reaction vessel. The schematic setup of the reaction system can be referred to our previous works [4]. The lamp emits mostly in the range 310–1000 nm, with the most intense lines at 303, 313, 366, 405, 436, 546, and 578 nm. The average light intensity of $2.15 \times 10^{-4} \pm 5.74 \times 10^{-5}$ einstein s^{-1} L^{-1} ($n = 18$) was measured by an actinometric technique [17]. Light control experiment was also performed to evaluate Cr(VI) reduction in the absence of HA. HA suspensions were periodically extracted and passed through a 0.2 μm pore-size membrane filter to collect the filtrates. Cr(VI) concentration in the filtrate was determined using a UV/VIS spectrophotometer (Varian Cary 50) at 540 nm after reaction with an 1,5-diphenylcarbazide indicator (DPC) [21]. The dark control was conducted when the light was turned off. Total chromium was determined using atomic absorption spectroscopy (AAS; Hitachi Z-2000) at $\ddot{y} = 359.3$ nm. The differences between total Cr and Cr(VI) concentrations obtained by AAS and DPC methods, respectively, were attributed to Cr(III).

3. Results and discussion

3.1. Mass distribution of each HA fraction

The HA fraction with the greatest molecular cutoff (i.e. $M_w > 100$ kDa) consists of 85.9% of the total HA mass recovered from the UF process. There was a dramatic decrease in the mass distribution of HA for 50–100 kDa, and 10–50 kDa had the lowest mass distribution (Table 1). The smallest molecular cutoff (i.e. $M_w < 10$ kDa) constituted 17.3% of the total HAs mass. The results indicate that the major mass distributions of HAs were within a narrow range of M_w, consistent with several previous studies using UF to fractionate HAs derived from different sources [22–24].

3.2. Characterizations of HA

3.2.1. Elemental analysis

The bulk HA sample derived from Yangmingshan peat soil had C, H, N and O contents of 51.3, 5.3, 2.5 and 38.5%, respectively (Table 1).
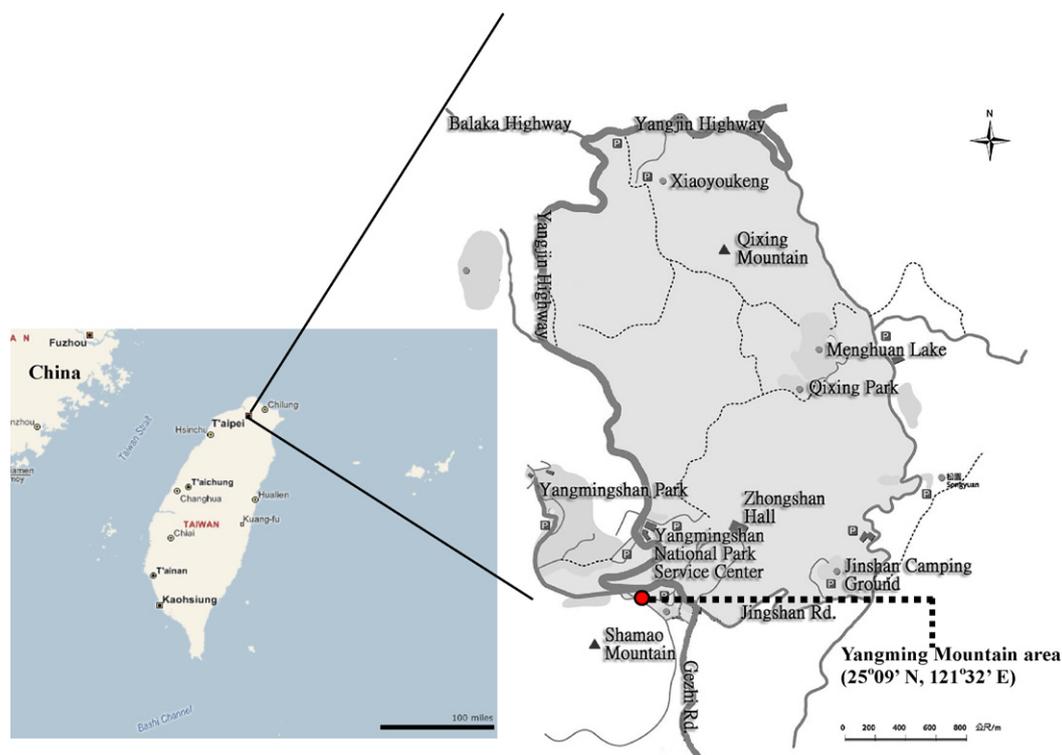
Fig. 1. Location of Yangmingshan peat soil collected from northern Taiwan.

With decreased M_w of HAs, the C and H contents of HAs decreased accompanied by an increase in O contents. The H/C atomic ratio decreased from 1.06 to 0.92, in contrast to the increased O/C atomic ratio from 0.53 to 0.60, when M_w of HAs decreased from >100 to <10 kDa. The polarity index [(N + O)/C] also increased with a lower M_w of HA (Table 1). It seems clear that the HAs became more aliphatic and less polar when the M_w of HAs became larger.

3.2.2. E_4/E_6 values

There was a significant increase in E_4/E_6 ratios of HA fractions with decreased M_w of HAs (Table 1). The E_4/E_6 ratio is widely used as an index of the chemical characteristics of HAs, such as particle sizes or M_w of humic substances [20]. Kang and Xing [25] reported a negative correlation between E_4/E_6 and M_w, and the E_4/E_6 ratio is generally <5 for greater M_w of HAs and is 6–18.5 for FA with lower M_w [26]. These results are consistent with our E_4/E_6 data for Yangmingshan HAs (Table 1). The remarkable changes of the E_4/E_6 values with various M_w of HA fractions demonstrated the success of fractionation of HAs in the current study.

3.2.3. Spectroscopic studies

FTIR spectra of each HA fraction exhibited a broad absorption peak at about 3300–3670 cm^{-1} (Fig. 2), indicating the stretching vibration of hydroxyl groups, such as phenolic groups, on HA [27,28]. Except for the FTIR spectrum of HA with an M_w of 10–50 kDa, each HA fraction, including bulk HA, had similar FTIR spectroscopic results (Fig. 2). However, there were some differences in the characteristic absorbance peaks among the HA fractions of various M_w. For instance, with decreased M_w of HAs, there was a slight increase at 3030, 1718 and 1240 cm^{-1}, corresponding to the aromatic C–H stretching, –C=O stretching of –COOH, and oscillation of O-containing groups on –COOH [27–30], respectively (Fig. 2). Conversely, the intensities of the peaks at 2917, 2849 and 1070 cm^{-1}, assigned to C–H/C–C stretching of aliphatic groups [29], decreased with lower M_w of HAs (Fig. 2). FTIR spectra indicate that the low M_w of HAs contained more aromatic C and carboxyl groups, consistent with the EA analysis.

The relative percentages of the peak area of the solid-state ^{13}C CP-MAS NMR spectra for HA fractions were estimated as proposed by Li et al. [30] (Table 2). Within the aliphatic C-region of 0–112 ppm, the C contents decreased from 44.8 to 42.8%, in contrast to an increase in aromatic C (112–163 ppm) and aromaticity, when M_w of HAs decreased from >100 to <10 kDa (Table 2). Total percentage of polar groups, calculated by summation of the regions of 50–112 and 145–215 ppm in NMR spectra, increased with a lower M_w of HA. NMR spectra results were consistent with the data of EA and FTIR analyses and with the previous report for fractionated HAs derived from different soils [23]. For instance, by extracting

Table 1
Yield, elemental compositions, atomic ratio, and E_4/E_6 values of different size fraction of humic acids (HA).

Sample	Yield (wt%)	C (%)	H (%)	N (%)	O (%)	H/C[a]	O/C	(N+O)/C	E_4/E_6[b]
HA (bulk)		51.3	5.3	2.5	38.5	1.25	0.56	0.60	5.63
>100 kDa	85.9 ± 3	53.3	4.4	1.5	37.3	1.06	0.53	0.55	3.23
50–100 kDa	3.6 ± 4	50.9	4.5	1.4	39.5	0.98	0.58	0.60	7.31
10–50 kDa	1.5 ± 5	–[c]	–	–	–	–	–	–	8.16
<10 kDa	17.3 ± 7	50.1	3.8	1.3	40.3	0.92	0.60	0.63	11.11

[a] H/C: atomic ratio of hydrogen to carbon. O/C: atomic ratio of oxygen to carbon. (N+O)/C: atomic ratio of sum of nitrogen and oxygen to carbon.
[b] E_4/E_6 of humic acid is the ratio of the absorbance at 465 nm to that at 665 nm.
[c] Not measured.
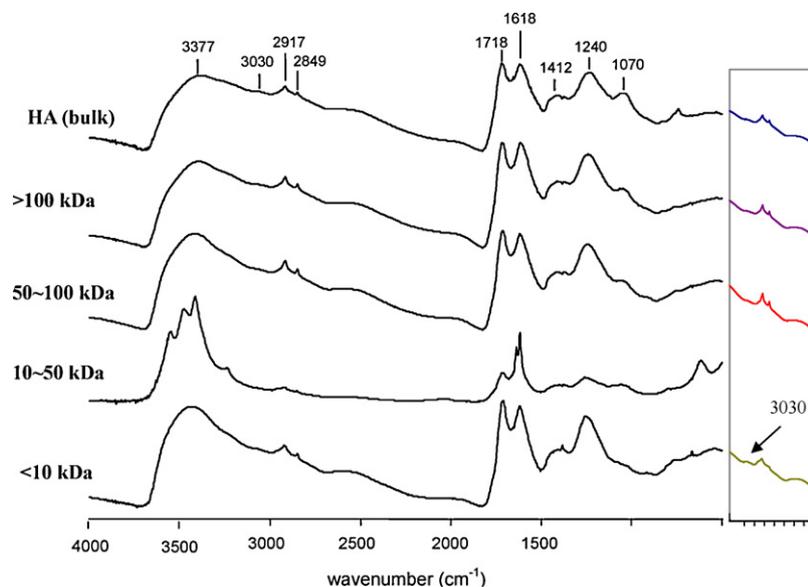
Fig. 2. FTIR spectra of Yangmingshan HAs of various molecular weights.

HA from a Pahokee peat (obtained from the IHSS), Li et al. [23] found that the low M_w had higher O/C atomic ratios and aromatic C, but lower H/C atomic ratios based on the chemical, spectroscopic, and pyrolysis–gas-chromatography–mass-spectrometry analyses. These results suggested that HA became more polar and aromatic with lower M_w. Since polar groups, such as carboxyl and phenolic groups, are the major activated sites for contaminants, we presume that the interactions of metals with HAs should be more efficient on HAs of lower M_w.

3.3. Cr(VI) removal on HA with various M_w

3.3.1. In darkness

Upon interaction of Cr(VI) with bulk HA (ca. $26 \pm 2 \, mg \, C \, L^{-1}$), about 8.8% of 0.1923 mM Cr(VI) was removed after 12 h of reaction at pH 1 (Fig. 3a). Within the same reaction time and experimental conditions, Cr(VI) removal on HA increased from 9.6 to 20.5% when the M_w of HA decreased from >100 to <10 kDa (Fig. 3b). The kinetic removal of Cr(VI) followed second-order reaction kinetics with rate constants of 5×10^{-4} to $8 \times 10^{-4} \, mM^{-1} \, min^{-1}$, depending on the M_w of HAs; and low M_w of HAs was more feasible for the removal of Cr(VI) from solutions. Since lower M_w HAs contained more aromatic C and carboxyl groups [31], the slight increase of Cr(VI) removal on a lower M_w HAs may be related to its higher aromatic and polar C contents (details below). Generally, Cr(VI) interaction with HA was slow in darkness, consistent with the report of Wittbrodt and

Palmer [11] who found that the complete reduction of 0.02 mM Cr(VI) on HA required tens of days.

There was a huge decrease in Cr(VI) removal on HAs when the solution pH was raised from 1 to 3 (data not shown). Only 3.3% of added Cr(VI) was removed even when the lowest M_w of HAs was used, and there was no discernible Cr(VI) removal at pH 5. The results demonstrate that Cr(VI) removal on HAs was pH-dependent and greatly inhibited at a higher pH, consistent with the report of Wittbrodt and Palmer [11]. Cr(VI) removal can be a combinative result of the adsorption and reduction of Cr(VI) on HA. To determine which of these two processes dominated Cr(VI) removal, 0.1 M KH_2PO_4 was used to extract adsorbed Cr(VI) [32], and the proportions of Cr(VI) reduction on HA were calculated based on Eqs. (1) and (2).

$$\begin{aligned}[Cr(VI)]_{removal} &= [Cr(VI)]_{initial} - [Cr(VI)]_{in \, solution} \\ &= [Cr(VI)]_{adsorption \, on \, HA} + [Cr(VI)]_{reduction}\end{aligned} \quad (1)$$

$$[Cr(VI)]_{extraction} = [Cr(VI)]_{adsorption \, on \, HA} + [Cr(VI)]_{in \, solution} \quad (2)$$

The amount of Cr(VI) adsorbed on HA can be calculated by subtracting the Cr(VI) concentration in solution from that obtained by K_2HPO_4/KH_2PO_4 buffer (P) extraction (Eq. (2)). Cr(VI) reduction is then obtained by subtracting the adsorbed Cr(VI) from the overall Cr(VI) removal (Eq. (1)). About 3.5, 2.6 and 2.1% of Cr(VI) was adsorbed on HAs with M_w of >100, 50–100 and <10 kDa, respectively, at 12 h reaction time at pH 1, and <1% of added Cr(VI) was adsorbed on each HA fraction at pH 3. The results demonstrated that

Table 2
Integration results of solid-state ^{13}C NMR spectra of different size of humic acids.

Sample	Distribution of C chemical shift (%)				Aliphatic C[a]	Polar[b]	Aromaticity[c]
	0–50 ppm	50–112 ppm	112–163 ppm	163–190 ppm	C (%)	C (%)	(%)
	alkyl	O-alkyl	aromatic	carboxyl			
HA (bulk)	22.1	26.1	28.3	14.0	48.2	45.7	37.0
>100 kDa	21.9	22.9	33.5	12.3	44.8	42.5	42.8
50–100 kDa	20.2	22.9	35.1	14.0	43.1	43.9	44.9
10–50 kDa	18.3	25.3	35.5	14.5	43.6	45.8	44.9
<10 kDa	14.2	28.6	36.0	15.8	42.8	50.6	45.7

[a] Aliphatic C: total aliphatic carbon region (0–112 ppm).
[b] Polar C: total polar C region (50–112 and 145–215 ppm).
[c] Aromaticity was calculated by expressing aromatic C (112–163 ppm) as percentage of the aliphatic and aromatic regions (0–163 ppm).
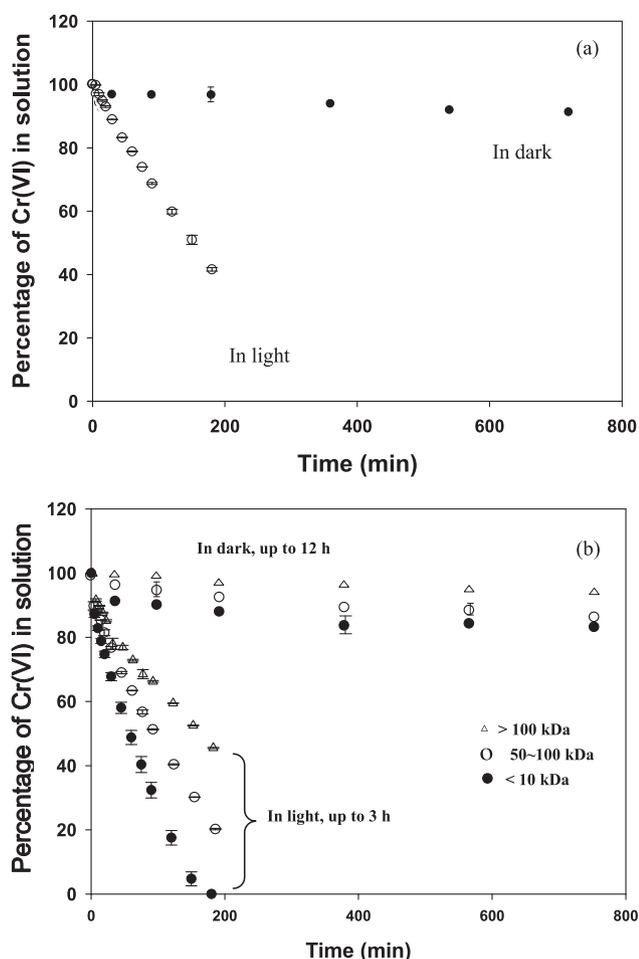
Fig. 3. Reduction of 0.1923 mM Cr(VI) on 26 mg C L^{-1}: (a) bulk HAs, and (b) HAs with various molecular weights at pH 1 in darkness or under illumination.

Cr(VI) reduction dominated Cr(VI) removal on HAs, i.e., HAs served mainly as electron donors instead of as adsorbents for Cr(VI).

Direct observations of the specific groups of HAs involved in Cr(VI) reduction are little reported in the literature. Nonetheless, other biomass, alcoholic, carboxyl and phenolic groups, which are commonly found in HA, have proven efficient reductants for Cr(VI) [32,33]. The formation of chromate ester was proposed as the first step in proceeding redox reactions [10]. That is, these authors suggested that some polar functional groups, such as hydroxyl and phenolic groups, were able to interact with Cr(VI) through the formation of chromate ester, a rapid and reversible process as described in the first reaction of Eq. (3). Following chromate ester formation, a slow electron-transfer from ester to Cr(VI) occurred, leading to Cr(VI) reduction (Eq. (3)). Since HAs contain these functional groups and the formation of chromate ester is reversible, we postulated that the adsorbed Cr(VI), defined by P extraction, may be partially derived from the chromate ester (Eq. (4)).

$$HCrO_4^- + ROH \overset{rapid}{\longleftrightarrow} [HCrO_4^- \cdot ROH] \overset{slow}{\longrightarrow} Cr(III) + decomposed\ organics$$

$$(3)$$

$$[HCrO_4^- \cdot ROH] \overset{extracted\ by\ P}{\longrightarrow} HCrO_4^- + H_2PO_4^- \cdot ROH \leftrightarrow H_2PO_4^- + ROH$$

$$(4)$$
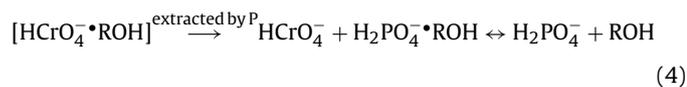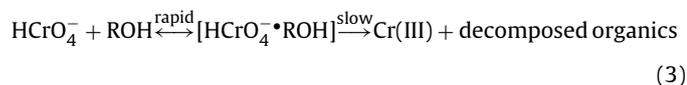
Once the Cr(VI) was converted to Cr(III), i.e., the slow redox reaction of Eq. (3), most of the redox products of Cr(III)

were released into solution (>97%) as calculated from Eqs. (5) and (6).

$$[Cr(III)]_{solution} = [Cr]_{in\ solution\ measured\ by\ AAS}$$
$$- [Cr(VI)]_{in\ solution\ measured\ by\ DPC} \qquad (5)$$

$$[Cr(VI)]_{adsorption} + [Cr(III)]_{adsorption}$$
$$= [Cr(VI)]_{initial} - [Cr]_{in\ solution\ measured\ by\ AAS} \overset{re\text{-}arrange}{\longrightarrow}$$
$$[Cr(III)]_{adsorption} = [Cr(VI)]_{initial} - [Cr]_{in\ solution} - [Cr(VI)]_{adsorption} \qquad (6)$$

Accordingly, in darkness, the slow disappearance of Cr(VI) upon its reaction with HA was due to Cr(VI) reduction. Since Cr(VI) reduction consumed protons (Eq. (7)) [32], an elevation of solution pH created an unfavorable environment for Cr(VI) reduction. In addition, the increase of negative charges on both reactants, i.e., Cr(VI) and HAs, with an increase of solution pH may inhibit electron transfer, leading to slow reduction of Cr(VI) on HA.

$$HCrO_4^- + 7H^+ + 3e^- \Leftrightarrow Cr^{3+} + 4H_2O \qquad (7)$$
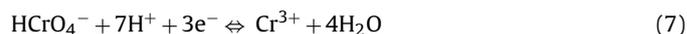
3.3.2. Under illumination

Upon exposure to light, Cr(VI) removal on each M_w fraction of HAs was greatly enhanced (Fig. 3). For instance, 0.1923 mM Cr(VI) was completely removed by the lowest M_w of HAs (i.e. <10 kDa) after 3 h of reaction under illumination at pH 1 (Fig. 3b). Even the highest M_w of HAs removed >57% of initially added Cr(VI) within the same reaction time and experimental conditions. Cr(VI) removal on each M_w of HAs followed first-order kinetics with rate constants from 5.0×10^{-4} to 1.3×10^{-2} min^{-1} (Table 3). The change in the kinetic model from second- to first-order suggested that the reaction mechanism of Cr(VI) reduction by HA under a light condition was different from that of dark. That is, a photo-induced reaction participates the conversion of Cr(VI) by HA (please see below). Low pH associated with low M_w of HAs was more favorable for Cr(VI) removal. The light-promoted and rapid disappearance of Cr(VI) was due to increased Cr(VI) reduction on various M_w fractions of HAs because only slight Cr(VI) (less than 1%) could be reduced in the absence of HA based on the control experiment. In addition, no adsorbed Cr(VI), evaluated by P extractive processes, was found under illumination (as calculated by Eqs. (1) and (2)).

HAs, FAs and DOM have been reported to be capable of reducing Cr(VI) at low pH, and the redox reaction can be enhanced under illumination [10,17]. Macromolecules of HAs, bearing olefinic, aromatic, and phenolic–semiquinone–quinone structures of a wide spectrum with various functional groups and chromophores, are capable of absorbing electromagnetic radiation [34]. Upon absorption of light energy, the photophysical and photochemical properties of HAs, e.g. the intensities of chemiluminescence and fluorescence emission, are correspondingly changed [35]. Lipski et al. [35] further suggested that the changes are intrinsically associated with the generation of excited states and reactive oxygen species such as $O_2^{\bullet-}$ and H_2O_2. In the current study, we also found that ca. 21.9 μM H_2O_2, measured by photometric method [36], could be produced upon exposure HA to the light at 2 h in the absence of Cr(VI). Therefore, we speculated that photo-induced formation of superoxide radicals and H_2O_2 (Eqs. (8)–(12), [17,33,35,36]) may be responsible for the rapid Cr(VI) reduction on bulk HA (Fig. 3a) because these peroxide compounds are efficient reductants for Cr(VI) (Eqs. (13) and (14) [33,36]).

$$R + O_2 + h\nu \rightarrow R^{\bullet+} + O_2^{\bullet-} \qquad (8)$$

$$R^{\bullet+} + O_2 \rightarrow R^{2+} + O_2^{\bullet-} \qquad (9)$$

$$O_2^{\bullet-} + H_2O \rightarrow HO_2^{\bullet} + OH^- \qquad (10)$$

$$O_2^{\bullet-} + HO_2^{\bullet} + H^+ \rightarrow H_2O_2 + O_2 \qquad (11)$$
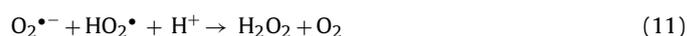
Table 3
First-order rate constant (k) for the photo-reduction of Cr(VI) on HA with various molecule weights as influenced by the pH.

pH	HA (bulk)		HA (>100 kD)		HA (50–100 kD)		HA (<10 kD)	
	k (min^{-1})	r^2	k (min^{-1})	r^2	k (min^{-1})	r^2	k (min^{-1})	r^2
1	$4.3 \times 10^{-3} \pm 3 \times 10^{-4}$	0.99	$3.8 \times 10^{-3} \pm 2 \times 10^{-5}$	0.98	$6.4 \times 10^{-3} \pm 1 \times 10^{-4}$	0.99	$1.3 \times 10^{-2} \pm 5 \times 10^{-4}$	0.98
3	$1.5 \times 10^{-3} \pm 1 \times 10^{-4}$	0.99	$1.2 \times 10^{-3} \pm 5 \times 10^{-5}$	0.99	$2.4 \times 10^{-3} \pm 2 \times 10^{-5}$	0.99	$6.6 \times 10^{-3} \pm 2 \times 10^{-4}$	0.99
5	$7.0 \times 10^{-4} \pm 1 \times 10^{-5}$	0.98	$5.0 \times 10^{-4} \pm 3 \times 10^{-5}$	0.97	$8.0 \times 10^{-4} \pm 1 \times 10^{-5}$	0.95	$6.1 \times 10^{-3} \pm 1 \times 10^{-4}$	0.94

$$O_2^{\bullet -} + H_2O \rightarrow H_2O_2 + 2OH^- \tag{12}$$

where R indicates photo-inducible organic groups in bulk HAs.

$$O_2^{\bullet -} + HCrO_4^- + 5H^+ \rightarrow 3H_2O + Cr^{3+} + 3/2O_2 \tag{13}$$

$$3/2H_2O_2 + HCrO_4^- + 4H^+ \rightarrow 4H_2O + Cr^{3+} + 3/2O_2 \tag{14}$$
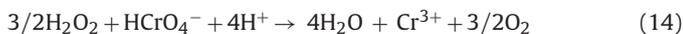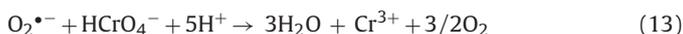
Similarly to the results obtained in darkness, low-M_w HAs exhibited an apparently higher reductive ability of Cr(VI) compared with those for high-M_w HAs when light was applied. The reasons are threefold: (1) aromatic moieties, including quinones with carbonyl-type chromophores, dominated the formation of C-centered radicals upon the absorption of UV irradiation [37]. Since low-M_w HAs contained more aromatic domains, we expected that more reactive groups (i.e. $O_2^{\bullet -}$ and H_2O_2) may be produced upon exposure of the low-M_w HAs to light. As a result, Cr(VI) reduction was greatly enhanced. (2) As mentioned previously, the formation of chromate-phenol ester is rapid; however, the slow electron-transfer from phenol to Cr(VI) is rate-limiting for Cr(VI) reduction [10]. In the presence of light, the light energy may overcome the energy gap for rapid electron transfer between these two reactants, and thus, significantly elevated Cr(VI) reduction, decreasing the life-time of adsorbed Cr(VI) in the ester phase. (3) In an aerobic environment, photo-induced formation of C-centered organic radicals (Eq. (15)) would add O_2 to form a peroxy radical (Eq. (16)) [38].

$$R^1R^2C + h\nu \rightarrow R^1R^2C^\bullet \tag{15}$$

$$R^1R^2C^\bullet + O_2 \rightarrow R^1R^2C(O_2)^\bullet \tag{16}$$
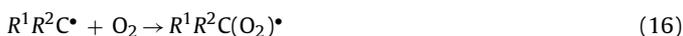
When a polar substituent of OH or CO_2^- (i.e. a heteroatom with a non- or anti-bonding electron pair) exists in the peroxy radical, the peroxy radical will become unstable and decay within a few milliseconds to yield the corresponding products, such as aldehyde, ketone, acid, and superoxide radical (Eq. (17)) [38]. Thus, low-M_w HA having a higher polar group (comparable to that of high-M_w HA) may lead to a rapid conversion of peroxyl radical to superoxide radical (Eq. (17)) for subsequent Cr(VI) reduction (Eq. (13)).

$$R^1R^2(OH)C(O_2)^\bullet \rightarrow R^1R^2CO + H^+ + O_2^{\bullet -} \tag{17}$$
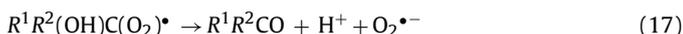
In the environment, the presence of trace elements such as Fe may promote Cr(VI) photo-reduction by HA; nonetheless, no Fe were detected in the current systems. Therefore, the possible contributions of trace elements to Cr(VI) reduction in the presence of HA can be ruled out. However, it merits further study to clarify the influences of trace elements on Cr(VI) reduction on various M_w of HA.

3.4. Spectroscopic analyses of Cr(VI)-treated HAs

To investigate the changes of HA components upon their interactions with Cr(VI), a series of Cr(VI) concentrations up to 9.615 mM were applied to allow the spectroscopic analyses of the changes of HA structures upon their oxidation by Cr(VI). Control experiments indicated that a direct complexation of Cr(III) with HA would lead to a slight effect on the spectroscopic results. Therefore, the significant changes in HA structures shown in FTIR and NMR spectra upon the addition of Cr(VI) were due to oxidation by Cr(VI).

Along with the reduction of Cr(VI), several major functional groups of HAs were correspondingly changed. For instance, FTIR spectra showed a strong absorption peak at 1718 cm^{-1}, assigned to carboxyl groups, which gradually decreased with increased Cr(VI) concentrations (Fig. 4). The results demonstrate that the carboxylic groups of HAs might be oxidized by Cr(VI) or complex with Cr(III), leading to a shift of the –C=O band to a lower frequency at ca. 1639–1648 cm^{-1} [39]. This shift broadened the strong characteristic peak of carbonyl group at 1618 cm^{-1} (Fig. 4). In addition, the peaks at 1412 and 1240 cm^{-1}, indicating O–H bending vibration of carboxylic groups and simultaneous oscillation of C–O/O–H groups of –COOH, respectively, also decreased when Cr(VI) was added. Accompanied with a decrease of carboxylic groups, the peaks at 1240 and 1412 cm^{-1} shifted to 1264 and 1383 cm^{-1}, respectively, which may be attributed to the adsorption of Cr(III) on the residual carboxylic groups (Fig. 4) [39]. In contrast to the changes of polar functional groups, the peaks at 2919, 2849 and 1070 cm^{-1}, representative of C–H/C–C stretching of aliphatic groups, remained almost unchanged which suggested that the specific sites of HAs with non-polar properties and enriched in aliphaticity were more resistant to the attack of Cr(VI).

As mentioned previously, both oxidation and Cr(III) binding on carboxylic groups would result in an attenuation of absorption peaks at 1718 and 1240 cm^{-1}. To further evaluate the effect of Cr(III) binding on the decrease in these two absorption peaks, 1.923 mM Cr(III) was used to interact directly with HAs and the
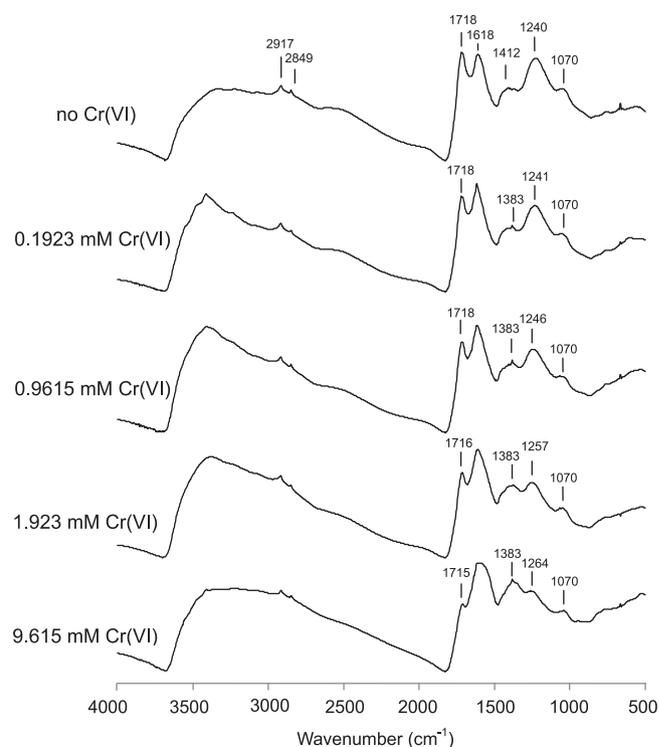
Fig. 4. FTIR spectra of Yangmingshan HAs pre-treated with different Cr(VI) concentrations.
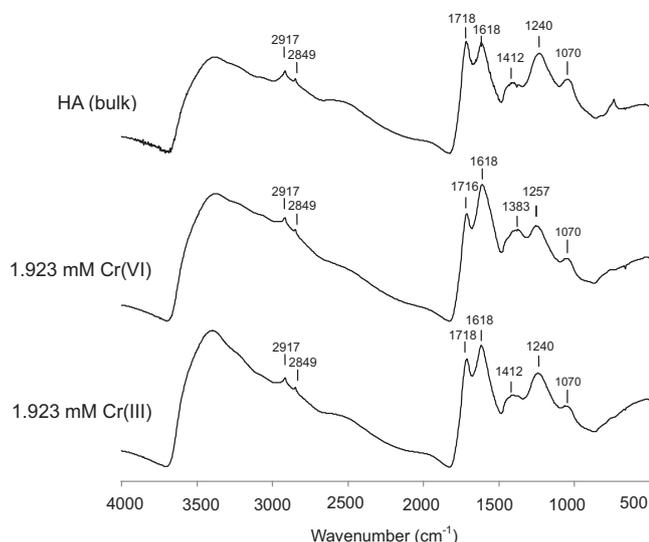
Fig. 5. FTIR spectra of original, and Cr(III)- and Cr(VI)-treated HAs.

Fig. 6. ^{13}C NMR spectra of HAs pre-treated with Cr(VI) up to 9.615 mM.

FTIR was monitored (Fig. 5). Although there was a slight decrease in the absorption peaks at 1718 and 1240 cm^{-1} with addition of Cr(III), the changes were small compared to HA samples treated with Cr(VI). In addition, the adsorption of Cr(III) on HAs caused only a slight shift of the peak at 1412–1383 cm^{-1} (Fig. 5). These spectroscopic results suggested that Cr(III) binding was not the only process resulting in the decrease of absorption peaks of carboxylic groups on Cr(VI)-treated HAs. The oxidation of HAs by Cr(VI) might also contribute to the gradual decrease of the absorption peaks at 1718 and 1240 cm^{-1}. Corresponding with the decrease of carboxylic signals on FTIR spectra, the peaks at 1618 and 1383 cm^{-1}, respectively, were concurrently broadened and increased due to Cr(III) binding (Fig. 4).

NMR spectra demonstrated that the oxidation of HAs by Cr(VI) occurred mainly at aromatic domains with polar properties (Fig. 6) and demonstrated again the strong interactions of Cr(VI) with low-M_w HAs. Moreover, non-polar aliphatic C of HAs (0–50 ppm) [19,25] seemed to resist oxidation by Cr(VI); nonetheless, polar functional groups within the aliphatic C region of HAs (50–112 ppm) [19] still exhibited chemical reactivity with Cr(VI) (Fig. 6). These results support the redox reactions (Eqs. (3) and (15–17)) and address that the polar sites of HAs dominate Cr(VI) reduction. NMR results did not conclude that O-containing aromatic and aliphatic C were completely oxidized by Cr(VI) because a small amount of aromatic and O-containing C still existed on the basis of the integration results of NMR spectra (data not shown). That is, a portion of aromatic domains of HA may be converted to small organic molecules upon their oxidations by Cr(VI) instead of formation of CO$_2$. Thus, the residual O-containing groups could contribute to the absorption peaks shown in FTIR spectra.
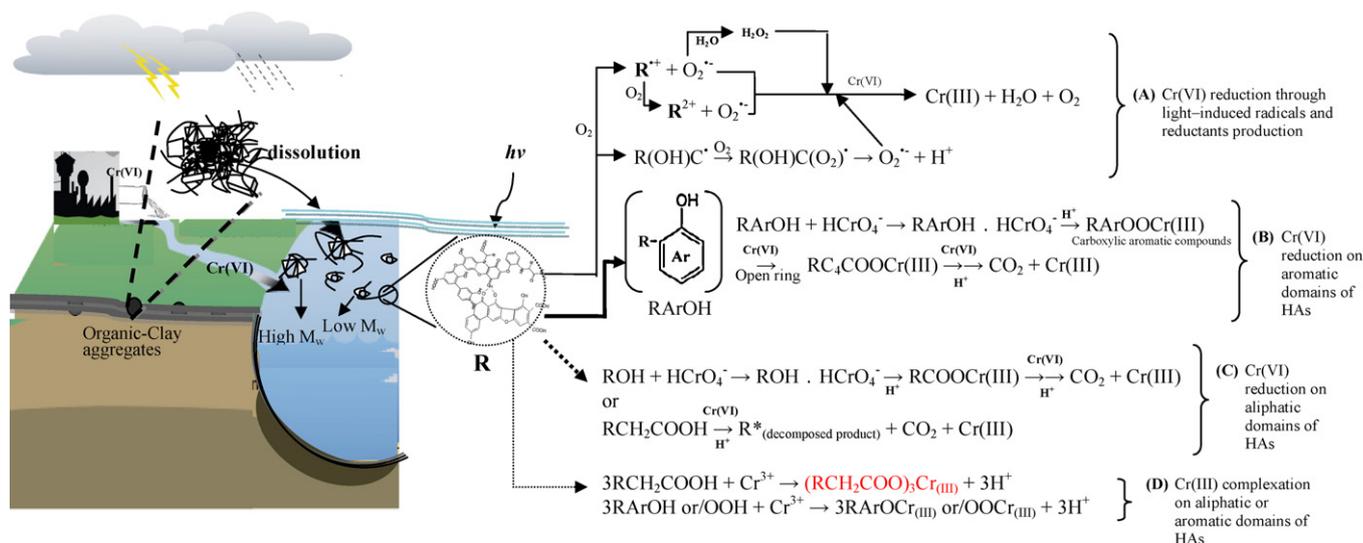
Fig. 7. The schematic descriptions of Cr(VI) removal on the components of HAs.

4. Conclusions

In the present study, Yangmingshan HAs were fractionated into different M_w, and low-M_w HAs exhibited a higher aromaticity and polarity than high M_w. The aromatic domains of HAs with polar functional groups, such as phenolic and carboxylic groups, are the major sites participating in Cr(VI) reduction (Fig. 7, pathway B). Spectroscopic results indicated that polar aliphatic C was also involved in Cr(VI) reduction (Fig. 7, pathway C). Therefore, soil substances with higher aromaticity and polarity may possess great potential for Cr(VI) removal. Upon interaction of HAs with water, a portion of HAs are subject to hydrolysis or dissolution, releasing loosely bonded organic and inorganic compounds and making the HA polymer charged similarly to polyelectrolytes. If the hydrolytic products and the materials trapped in crosslinked network of HA enriched with aromatic and polar groups, the derived DOC may contain a number of activated sites for Cr(VI). Once the DOC is transferred to a sunlit environment, a photo-catalytic process can be initiated near the polar positions of DOC, leading to the production of H_2O_2 or superoxide radicals, for rapid Cr(VI) reduction (Fig. 7, pathway A). The redox product of Cr(III) is then either released in the solution or adsorbed on the carboxylic or other polar groups of HAs (Fig. 7, pathway D).

Acknowledgements

References

[1] M. Farrell, D.L. Jones, Use of composts in the remediation of heavy metal contaminated soil, J. Hazard. Mater. 175 (2010) 575–582.

[2] C.K. Ahn, S.H. Woo, J.M. Park, Surface solubilization of phenanthrene by surfactant sorbed on soils with different organic matter contents, J. Hazard. Mater. 177 (2010) 799–806.

[3] Y. Gao, W. Xiong, W. Ling, X. Wang, Q. Li, Impact of exotic and inherent dissolved organic matter on sorption of phenanthrene by soils, J. Hazard. Mater. 140 (2007) 138–144.

[4] Y.M. Tzou, C.L. Hsu, C.C. Chen, J.H. Chen, J.J. Wu, K.J. Tseng, Influence of inorganic anion on Cr(VI) photo-reduction in the presence of ferric ion, J. Hazard. Mater. 156 (2008) 374–380.

[5] J.P. Aguer, O. Trubetskaya, O. Trubetskoj, C. Richard, Hotoinductive properties of soil humic acids and their fractions obtained by tandem size exclusion chromatography-polyacrylamide gel electrophoresis, Chemosphere 44 (2001) 205–209.

[6] M. Schnitzer, Soil organic matter-the next 75 years, Soil Sci. 151 (1991) 41–58.

[7] C. Richard, G. Guyot, A. Rivaton, O. Trubetskaya, O. Trubetskoj, L. Cavani, C. Ciavatta, Spectroscopic approach for elucidation of structural peculiarities of Andisol soil humic acid fractionated by SEC-PAGE setup, Geoderma 142 (2007) 210–216.

[8] I. Christl, R. Kretzschmar, Relating ion binding by fulvic and humic acids to chemical composition and molecular size. 1. Proton binding, Environ. Sci. Technol. 35 (2001) 2505–2511.

[9] O. Trubetskaya, O. Trubetskoj, G. Guyot, F. Andreux, C. Richard, Fluorescence of soil humic acids and their fractions obtained by tandem size exclusion chromatography-polyacrylamide gel electrophoresis, Org. Geochem. 33 (2002) 213–220.

[10] P.R. Wittbrodt, C.D. Palmer, Reduction of Cr(VI) in the presence of excess soil fulvic acid, Environ. Sci. Technol. 29 (1995) 255–263.

[11] P.R. Wittbrodt, C.D. Palmer, Reduction of Cr(V1) by soil humic acids, Euro. J. Soil Sci. 47 (1996) 151–162.

[12] Y.M. Tzou, R.H. Loeppert, M.K. Wang, Light-catalyzed chromium(VI) reduction by organic compounds and soil minerals, J. Environ. Qual. 32 (2003) 2076–2084.

[13] Y.M. Tzou, M.K. Wang, R.H. Loeppert, Organic ligand-enhanced photochemical reduction and immobilization of chromium(VI) on TiO₂ particles in acidic aqueous media, Soil Sci. 169 (2004) 413–422.

[14] M.A. Turner, R.H. Rust, Effects of chromium on growth and mineral nutrition of soybeans, Soil Sci. Soc. Am. Proc. 35 (1971) 755–758.

[15] M. Ajmal, A.A. Nomani, A. Ahmad, Acute toxicity of chrome electroplating wastes to microorganisms: adsorption of chromate and chromium(VI) on mixture of clay and sand, Water, Air, Soil Pollut. 23 (1984) 119–127.

[16] J. Guertin, J.A. Jacobs, C.P. Avakian, Chromium(VI) Handbook, CRC Press, New York, 2005.

[17] M. Gaberell, Y.P. Chin, S.J. Hug, B. Sulzberger, Role of dissolved organic matter composition on the photoreduction of Cr(VI) to Cr(III) in the presence of iron, Environ. Sci. Technol. 37 (2003) 4403–4409.

[18] C.L. Hsu, S.L. Wang, Y.M. Tzou, Photocatalytic reduction of Cr(VI) in the presence of NO₃⁻ and Cl⁻ electrolytes as influenced by Fe(III), Environ. Sci. Technol. 41 (2007) 7907–7914.

[19] Y.Y. Huang, S.L. Wang, J.C. Liu, Y.M. Tzou, R.R. Chang, J.H. Chen, Influences of preparative methods of humic acids on the sorption of 2,4,6-trichlorophenol, Chemosphere 70 (2008) 1218–1227.

[20] Y. Chen, N. Senesi, M. Schnitzer, Information provied on humic substances by E_4/E_6 ratios, Soil Sci. Soc. Am. J. 41 (1977) 352–358.

[21] A.D. Eaton, L.S. Clesceri, A.E. Greenberg, Standard Methods for the Examination of Water and Wastewater, 19th ed., American Public Health Association, Washington, DC, 1995.

[22] H.S. Shin, J.M. Monsallier, G.R. Choppin, Spectroscopic and chemical characterizations of molecular size fractionated humic acid, Talanta 50 (1999) 641–647.

[23] L. Li, Z. Zhao, W. Huang, P. Peng, G. Sheng, J. Fu, Characterization of humic acids fractionated by ultrafiltration, Org. Geochem. 35 (2004) 1025–1037.

[24] R. Benner, B. Biddanda, B. Black, M. McCarthy, Abundance, size distribution, and stable carbon and nitrogen isotopic compositions of marine organic matter isolated by tangential-flow ultrafiltration, Mar. Chem. 57 (1997) 243–263.

[25] S. Kang, B. Xing, Phenanthrene sorption to sequentially extracted soil humic acids and humins, Environ. Sci. Technol. 39 (2005) 134–140.

[26] J.A. Leenheer, Origin and nature of humic substances in the waters of the Amazon river basin, Acta Amazonica 10 (1980) 513–526.

[27] F.J. Stevenson, Humus Chemistry: Genesis, Composition, Reactions, second ed., John Wiley & Sons, New York, 1994.

[28] M. Giovanela, J.S. Crespo, M. Antunes, D.S. Adamatti, A.N. Fernandes, A. Barison, C.W.P. da Silva, R. Guegan, M. Motelica-Heino, M.M.D. Sierra, Chemical and spectroscopic characterization of humic acids extracted from the bottom sediments of a Brazilian subtropical microbasin, J. Mol. Struct. 981 (2010) 111–119.

[29] R. Bloom, J.A. Leenheer, in: M.H.B. Hayes, P. McCarthy, R.L. Malcolm, R.S. Swift (Eds.), Humic Substances: In Search of Structure, Jonh Wiley, New York, NY, USA, 1989, pp. 410–446.

[30] L. Li, W. Huang, P. Peng, G. Sheng, J. Fu, Chemical and molecular heterogeneity of humic acids repetitively extracted from a peat, Soil Sci. Soc. Am. J. 67 (2003) 740–746.

[31] J.N. Wang, A.M. Li, Y. Zhou, L. Xu, Study on the influence of humic acid of different molecular weight on basic ion exchange resin's adsorption capacity, Chin. Chem. Lett. 20 (2009) 1478–1482.

[32] Y.C. Lin, S.L. Wang, W.C. Shen, P.M. Huang, P.N. Chiang, J.C. Liu, C.C. Chen, Y.M. Tzou, Photo-enhancement of Cr(VI) reduction by fungal biomass of Neurospora crassa, Appl. Catal. B: Environ. 92 (2009) 294–300.

[33] L.C. Hsu, S.L. Wang, Y.C. Lin, M.K. Wang, P.N. Chiang, J.C. Liu, W.H. Kuan, C.C. Chen, Y.M. Tzou, Removal on fungal biomass of neurospora crassa: the importance of dissolved organic carbons derived from the biomass to Cr(VI) reduction, Environ. Sci. Technol. 44 (2010) 6202–6208.

[34] C.S. Uyguner, M. Bekbolet, Implementation of spectroscopic parameters for practical monitoring of natural organic matter, Desalination 176 (2005) 47–55.

[35] M. Lipski, J. Slawinski, D. Zych, Changes in the luminescent properties of humic acids induced by UV-radiation, J. Fluoresc. 9 (1999) 133–138.

[36] C.J. Lin, S.L. Wang, P.M. Huang, Y.M. Tzou, J.C. Liu, C.C. Chen, J.H. Chen, C. Lin, Chromate reduction by zero-valent Al metal as catalyzed by polyoxometalate, Water Res. 43 (2009) 5015–5022.

[37] K. Polewski, D. Slawinska, J. Slawinski, A. Pawlak, The effect of UV and visible light radiation on natural humic acid EPR spectral and kinetic studies, Geoderma 126 (2005) 291–299.

[38] C. Kormann, D.W. Bahnemann, M.R. Hoffmann, Photocatalytic production of H₂O₂ and organic peroxides in aqueous suspensions of TiO₂, ZnO, and desert sand, Environ. Sci. Technol. 22 (1988) 798–806.

[39] M.F. Sawalha, J.R. Peralta-Videa, G.B. Saupe, K.M. Dokken, J.L. Gardea-Torresdey, Using FTIR to corroborate the identity of functional groups involved in the binding of Cd and Cr to saltbush (Atriplex canescens) biomass, Chemosphere 66 (2007) 1424–1430.